ELSEVIER

Journal of Magnetism and Magnetic Materials 198–199 (1999) 698–702

Journal of magnetism and magnetic materials

Invited paper

X-ray scattering from magnetically and structurally rough surfaces

R.M. Osgood III[a,b], S.K. Sinha[c,*], J.W. Freeland[d], Y.U. Idzerda[d], S.D. Bader[a]

[a]*Materials Science Division, Argonne National Laboratory, 9700 So. Cass Ave., Argonne, IL 60439, USA*
[b]*Building 253, 3M Center, 3M Corporation, St. Paul, MN 55144, USA*
[c]*Advanced Photon Source, Experimental Facilities Division, Argonne National Laboratory, 9700 So. Cass Ave., Argonne, IL 60439, USA*
[d]*Materials Science Division, Naval Research Laboratory, Washington, DC 20379, USA*

Abstract

We present expressions for the resonant magnetic X-ray scattering (XRMS) by surfaces possessing roughness and analyze both the structural and magnetic roughness of a surface, as well as their correlation. We demonstrate that the leading contribution to the difference (ΔI) in the diffuse scattering between left- and right-circularly polarized light for a rough surface vanishes unless the structural and magnetic roughnesses are correlated, to leading order in the magnetization. The effects of magnetic domain structure and magnetic dead layers on the surface scattering are also discussed.

Keywords: X-ray resonant magnetic scattering; Surface roughness

The use of X-ray reflectivity and off-specular (diffuse) surface scattering has become increasingly popular over the last decade as a method for characterizing the roughness and surface morphology of thin films and multilayers [1]. While not being able to provide actual images of the surface, such techniques have complementary advantages, such as the ability to make global statistical characterization of the morphology of such surfaces and also to study buried interfaces in an in situ and non-destructive manner. However, the magnetic analogue of such experiments has received much less attention until recently. Roughness at a ferromagnetic interface is a critical parameter for technologically important magnetic multilayers exhibiting the Giant Magnetoresistance (GMR) effect; roughness on the length scale of the period of interlayer magnetic coupling has been shown to reduce the GMR [2,3]. The theory of specular reflectivity and grazing incidence diffraction from magnetic surfaces in the absence of roughness has been derived [4,5], and there have been some recent studies of surface magnetism in crystals and thin films using such techniques [6–12].

Non-resonant magnetic X-ray scattering yields scattered amplitudes some three orders of magnitude smaller than those of pure charge X-ray scattering [6]. However, if the photon energy is tuned to a transition involving magnetically split levels of a particular atom in the sample, the amplitudes for charge and magnetic scattering can be comparable [6,7,13]. Recent measurements of X-ray resonant magnetic scattering (XRMS) [8–10] have focused attention on the use of the surface specular and diffuse X-ray scattering to determine both the structural (i.e. charge) and magnetic roughnesses of magnetic thin films. In these experiments, the scattered intensity for incident helicity close to parallel and anti-parallel to the sample magnetization (set by an applied external field) was measured and their average I_{ave} taken to determine the 'structural roughness'; the 'magnetic roughness' was assumed to be found by taking the difference, ΔI. As we shall see below, this is not completely correct.

* Corresponding author.
E-mail address: sksinha@aps.anl.gov (S.K. Sinha)

0304-8853/99/$ – see front matter
PII: S0304-8853(98)01098-1

Our calculations are performed in the Born approximation (BA), so that the entire sample is treated as a perturbation. Let us first consider a single surface. Neglecting the variations of charge and magnetization density on atomic length scales, we may represent the charge and magnetization density as being constant inside the 'structural' and 'magnetic' surfaces, respectively.

In the BA, the matrix element for elastic scattering from a photon state ($\boldsymbol{k}_i, \mu$) to the state ($\boldsymbol{k}_f, \mu'$), where $\boldsymbol{k}_{i,f}$ are the incident and final wavevectors (with the same absolute magnitude) and μ, μ' are the corresponding polarization states, is given by the matrix element below:

$$\langle \boldsymbol{k}_f, \mu' | T | \boldsymbol{k}_i, \mu \rangle = -4\pi r_0 n_0 (\boldsymbol{e}^*(\mu') \cdot \boldsymbol{e}(\mu)) \int_S d^3 r \, e^{-i\boldsymbol{q}\cdot\boldsymbol{r}} - 4\pi n_m \Bigg[iB (\boldsymbol{e}^*(\mu') \times \boldsymbol{e}(\mu)) \cdot \boldsymbol{M}) \cdot \int_M d^3 r \, e^{-i\boldsymbol{q}\cdot\boldsymbol{r}} p(\boldsymbol{r}) + C(\boldsymbol{e}^*(\mu') \cdot \boldsymbol{M})(\boldsymbol{e}(\mu) \cdot \boldsymbol{M}) \cdot \int_M d^3 r \, e^{-i\boldsymbol{q}\cdot\boldsymbol{r}} \Bigg], \quad (1)$$

(the cross-section is found by taking the modulus squared and dividing by $16\pi^2$). We have used the formula for the scattering length for one species of resonant atom from Ref. [6]. Here $\boldsymbol{q} = \boldsymbol{k}_f - \boldsymbol{k}_i$, $\boldsymbol{e}_{i,f}$ represent the photon polarization vectors of the incident and final states, n_0 represents an *effective* electron number density (with the contribution from the resonant atoms modified to include the resonant magnetic terms), n_m is the number density of magnetic atoms, $\boldsymbol{M}$ is the local magnetization vector (defined within a domain), r_0 is the Thomson scattering length of the electron, and F_{1m} are the resonant matrix elements, divided by an energy denominator, defined for a dipole transition. In Eq. (1), $B = (1/M)(F^0_{11} - F^0_{1-1})$ and $C = (1/M^2)(2F^0_{10} - F^0_{11} - F^0_{1-1})$ (B and C are in general complex because of absorption). We neglect the much smaller non-resonant magnetic scattering contributions [13].

Because in the BA, one treats the entire sample as a perturbation, *we assume that the sample is composed of two parts: a charge and magnetic volume, which overlap considerably but which are in general separate entities due to the presence of magnetic dead layers, etc.* These two volumes will have different roughnesses in general, so that the integral of $e^{-i\boldsymbol{q}\cdot\boldsymbol{r}}$ over the charge and magnetic volumes will be different; these different volume integrals are labelled S and M. The function $p(\boldsymbol{r})$ takes on the value $+1(-1)$ for domains aligned parallel (anti-parallel) to the net magnetization. We further assume that the domain walls are normal to the average surface. A schematic of the reference frame is displayed in Fig. 1. [Note that our formulae are not restricted to scattering within the plane of incidence as shown, but for general $\boldsymbol{k}_f$].

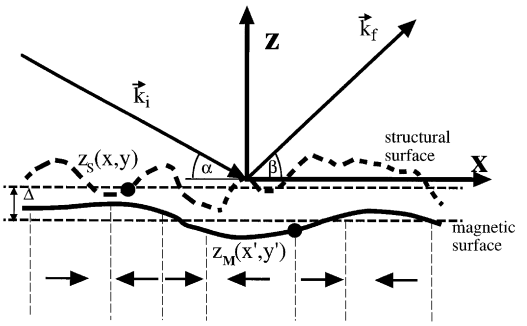

Fig. 1. Reference frame and sketch of the structural (charge) and magnetic interfaces, which in general can be separated from one another by an average amount Δ. Grazing angles of incidence (α) and scattering (β) are illustrated. Dotted lines indicate the locations of the average magnetic and structural surfaces.

Under these assumptions, the volume integrals in Eq. (1) can be transformed into surface integrals, [1] yielding:

$$\langle \boldsymbol{k}_f, \mu' | T | \boldsymbol{k}_i, \mu \rangle = -4i\pi r_0 n_0 (\boldsymbol{e}^*(\mu') \cdot \boldsymbol{e}(\mu)) \left(\frac{1}{q_z}\right) \times \iint dx\, dy\, e^{-iq_z Z_S(x,y)} e^{-i\boldsymbol{q}_\parallel \cdot \boldsymbol{\rho}} + 4\pi n_m (B (\boldsymbol{e}^*(\mu') \times \boldsymbol{e}(\mu)) \cdot \boldsymbol{M}) \left(\frac{1}{q_z}\right) \times \iint dx\, dy\, e^{-iq_z Z_M(x,y)} p(x,y)\, e^{-i\boldsymbol{q}_\parallel \cdot \boldsymbol{\rho}} + 4i\pi\, n_m (C (\boldsymbol{e}^*(\mu') \cdot \boldsymbol{M})(\boldsymbol{e}(\mu) \cdot \boldsymbol{M})) \left(\frac{1}{q_z}\right) \times \iint dx\, dy\, e^{-iq_z Z_M(x,y)} e^{-i\boldsymbol{q}_\parallel \cdot \boldsymbol{\rho}}, \quad (2)$$

where $\boldsymbol{q}_\parallel, \boldsymbol{\rho}$ are the in-plane components of $\boldsymbol{q}$ and $\boldsymbol{r}$, respectively, $z_S(x, y)$ and $z_M(x, y)$ are the heights of the structural and magnetic surfaces, respectively (see Fig. 1), and $p(x, y)$ is the magnetic domain function defined on the surface.

Using statistical averaging techniques with roughness fluctuations treated as a Gaussian random variable [1]), we obtain for the diffuse scattering cross-section:

$$\left.\frac{d\sigma}{d\Omega}\right|^{diff}_{k_i\mu \to k_f,\ \mu'} = PS_{ss}(\boldsymbol{q}) + RS^{(1)}_{mm}(\boldsymbol{q}) + QS_{mm}(\boldsymbol{q}) + TS_{sm}(\boldsymbol{q}) + T^* S^*_{sm}(\boldsymbol{q}), \quad (3)$$

$$P = r_0^2 n_0^2 \, |\boldsymbol{e}^*(\mu') \cdot \boldsymbol{e}(\mu)|^2, \quad (4)$$

$$Q = n_m^2 ([|C|^2 |(\boldsymbol{e}^*(\mu') \cdot \boldsymbol{M})(\boldsymbol{e}(\mu) \cdot \boldsymbol{M})|^2] - 2\, Re\, \{iBC^* \langle p \rangle [\boldsymbol{e}^*(\mu') \times \boldsymbol{e}(\mu)) \cdot \boldsymbol{M}] \times [(\boldsymbol{e}(\mu') \cdot \boldsymbol{M})(\boldsymbol{e}^*(\mu) \cdot \boldsymbol{M})]\}), \quad (5)$$

$$R = n_m^2 |B|^2 |\boldsymbol{e}^*(\mu') \times \boldsymbol{e}(\mu)) \cdot \boldsymbol{M}|^2, \tag{6}$$

$$T = r_0\, n_0 n_m([\boldsymbol{e}^*(\mu') \cdot \boldsymbol{e}(\mu)]\,[C^*(\boldsymbol{e}(\mu') \cdot \boldsymbol{M})(\boldsymbol{e}^*(\mu) \cdot \boldsymbol{M})] + iB^* \langle p \rangle [\boldsymbol{e}(\mu') \times \boldsymbol{e}^*(\mu)) \cdot \boldsymbol{M}]). \tag{7}$$

The terms $S_{ss}(\boldsymbol{q})$, etc. are defined as follows:

$$S_{ss}(\boldsymbol{q}) = \frac{A}{q_z^2} e^{-q_z^2\sigma_s^2} \iint dX\, dY\, (e^{q_z^2 C_{ss}(X,\,Y)} - 1) e^{-i\boldsymbol{q}_\parallel \cdot \boldsymbol{\rho}},$$

$$S_{sm}(\boldsymbol{q}) = \frac{A}{q_z^2} \langle p \rangle\, e^{-1/2 q_z^2(\sigma_s^2 + \sigma_M^2)} e^{-iq_z \Delta} f_m(q_z) \times \iint dX\, dY\, (e^{q_z^2 (C_{SM}(X,\,Y)} - 1) e^{-i\boldsymbol{q}_\parallel \cdot \boldsymbol{\rho}},$$

$$S_{mm}^{(1)}(\boldsymbol{q}) = \frac{A}{q_z^2} e^{-q_z^2\sigma_m^2} |f_m(q_z)|^2 \iint dX\, dY\, (e^{q_z^2 C_{MM}(X,\,Y)} - 1) \times e^{-i\boldsymbol{q}_\parallel \cdot \boldsymbol{\rho}} \gamma_m(X, Y),$$

$$S_{mm}(\boldsymbol{q}) = \frac{A}{q_z^2} e^{-q_z^2\sigma_m^2} |f_m(q_z)|^2 \iint dX\, dY\, (e^{q_z^2 C_{MM}(X,\,Y)} - 1) e^{-i\boldsymbol{q}_\parallel \cdot \boldsymbol{\rho}}, \tag{8}$$

where the integrals are taken over all possible in-plane distances $\boldsymbol{\rho} = (X, Y)$ separating the projection of a point on the appropriate surface from an arbitrary point or origin (0, 0), A is the area of the surface, $\sigma_{S,\,M}$ are the rms values of structural and magnetic roughnesses at the surface, Δ is the average separation of these two surfaces (see Fig. 1) (i.e., a magnetically dead layer), and C_{SS}, C_{MM}, and C_{SM} are structural–structural (SS), magnetic–magnetic (MM), and structural–magnetic (SM) correlation functions, respectively, for the roughness about the average surface. The function $f_m(q_z)$ is a form factor that takes into account the graded nature of the magnetic surface in the z-direction. The function $\gamma_m(X, Y)$ is the two-dimensional domain correlation function across the surface. Finally, $\langle p \rangle$ represents the global average of $p(X, Y)$ over all domains.

To allow for the fact that $C_{\xi_S} \to 0$ at large $\boldsymbol{\rho}$, we have substrated 1 from the arguments of the Fourier transforms in Eq. (8), thus omitting the specular contributions, which yield terms proportional to $4\pi^2\delta(q_x)\delta(q_y)$ arising from the Fourier transform. Strictly speaking, the Fourier transform of $\gamma_m(X, Y)$ is not a delta function, but if the domain size is larger than the X-ray coherence length, this term can be taken as being specular. From the delta function contributions, we may derive in the usual manner expressions for the specular reflectivities in the BA [1]:

$$|R|^2_{\mu \to \mu'} = \frac{16\pi^2}{q_z^4}[Pe^{-q_z^2\sigma_s^2} + (Q + R)e^{-q_z^2\sigma_m^2} + (Te^{iq_z\Delta} + T^* e^{-iq_z\Delta}) e^{-\frac{1}{2}q_z^2(\sigma_s^2 + \sigma_m^2)}]. \tag{9}$$

For values of q_z much larger than those involving total reflection, these expressions reduce to those deduced for charge and magnetic reflectivities for smooth surfaces, except for the Debye–Waller factors involving σ_S and σ_M. If $\langle p \rangle$ is small, then the effect of second order terms in $\boldsymbol{M}$ can be relatively significant. We note also that the averages over the surface are actually to be done over the coherence area of the X-ray beam along the x-axis, and much smaller along the y-axis (see Fig. 1)), so that if the magnetic domains are larger than this, we may consider the scattering as an incoherent superposition of that coming from single domains and simply set $\langle p \rangle = \gamma(X, Y) = 1$, ignoring domain effects. If this is not the case, we note that $S_{mm}^{(1)}(\boldsymbol{q})$ contains the convolution (in $\boldsymbol{q}_\parallel$) of $S_{mm}(\boldsymbol{q})$ with the Fourier transform of $\gamma_m(X, Y)$.

We now give explicit expressions for a simplified but common case, namely where $\boldsymbol{k}_i, \boldsymbol{k}_f$ are both in the x–z plane (i.e., no out-of-plane scattering) and $\boldsymbol{M} \| \hat{x}$ (see Fig. 1). The possible polarization states are then $\sigma\,(\boldsymbol{e}(\sigma)$ is the unit vector along the y-axis for both $\boldsymbol{k}_i$ and $\boldsymbol{k}_f$), $\pi(\boldsymbol{e}(\pi) = -\hat{y} \times \frac{\boldsymbol{k}_i}{|\boldsymbol{k}_i|}, \boldsymbol{e}(\pi') = -\hat{y} \times \frac{\boldsymbol{k}_f}{|\boldsymbol{k}_f|})$ and circular polarization of the incident beam of either sense: $\boldsymbol{e}_\pm = \frac{1}{\sqrt{2}}\boldsymbol{e}(\sigma) \pm i\boldsymbol{e}(\pi)$. The grazing angles of incidence and scattering (α, β) are indicated on Fig. 1. From Eq. (7), we obtain:

$$\left.\frac{d\sigma^{diff}}{d\Omega}\right|_{\sigma \to \sigma} = r_0^2 n_0^2 S_{ss}(\boldsymbol{q}), \tag{10}$$

$$\left.\frac{d\sigma^{diff}}{d\Omega}\right|_{\pi \to \pi} = r_0^2 n_0^2 \cos^2(\alpha + \beta) S_{ss}(\boldsymbol{q}) + n_m^2 |C|^2 \times M^4 \sin^2\alpha \sin^2\beta\, S_{mm}(\boldsymbol{q}) + 2r_0 n_m M^2 \cos(\alpha + \beta) \sin\alpha \sin\beta \times \mathrm{Re}(C^* S_{sm}(\boldsymbol{q}) n_0), \tag{11}$$

$$\left.\frac{d\sigma^{diff}}{d\Omega}\right|_{\sigma \to \pi} = n_m^2 |B|^2 M^2 \cos^2\beta\, S_{mm}^{(1)}(\boldsymbol{q}), \tag{12}$$

$$\left.\frac{d\sigma^{diff}}{d\Omega}\right|_{\pi \to \sigma} = n_m^2 |B|^2 M^2 \cos^2\alpha\, S_{mm}^{(1)}(\boldsymbol{q}). \tag{13}$$

For circularly incident polarization without polarization analysis for the outgoing beam, we have

$$\left(\frac{d\sigma}{d\Omega}\right)_\pm = \frac{1}{2}\left(\left.\frac{d\sigma}{d\Omega}\right|_{\sigma \to \sigma} + \left.\frac{d\sigma}{d\Omega}\right|_{\pi \to \pi} + \left.\frac{d\sigma}{d\Omega}\right|_{\sigma \to \pi} + \left.\frac{d\sigma}{d\Omega}\right|_{\pi \to \sigma}\right) \pm \mathrm{Re}(Bn_0^*)\,[\cos\alpha + \cos\beta(\alpha + \beta)] \times r_0 n_m M \langle p \rangle S_{sm}(\boldsymbol{q}) \mp \mathrm{Re}\, 2(B^*C) \sin\beta \sin\alpha \cos\beta \langle p \rangle n_m^2 M^3 S_{mm}(\boldsymbol{q}), \tag{14}$$

where, as before, we have assumed that the domain size is larger than the X-ray coherence length.

From Eq. (14), it is obvious that the leading term in the diffuse scattering difference ΔI between right- and left-circularly polarized light is a term that depends on both the structural and magnetic surfaces. If the structural and magnetic surfaces are completely uncorrelated (i.e., $C_{SM}(X, Y) = 0$) then $S_{sm}(\boldsymbol{q})$ vanishes, and ΔI has no diffuse term to leading order in M, as can be seen from Eq. (14) by taking the difference of the diffuse cross-section for the two different handednesses of the circular polarization. Often, instead of reversing the sense of polarization of the incident photon beam, $\boldsymbol{M}$ is reversed instead. This can be seen to have the same effect on $\Delta I = (I_+ - I_-)$ by simply reversing the sign of B in th ese expressions. We also note that, if there is a finite magnetically dead layer, it will in principle manifest itself through oscillations of period $2\pi/\Delta$ in both ΔI and in $\Delta|R|^2$, (these oscillations may be difficult to observe if the overall roughness is too large or the magnetic interface too diffuse). In principle, these oscillations will be present in the $\pi \to \pi$ scattering as well, but will probably be masked by the much larger charge scattering. Note that if the dead layer is only several Å thick, one must measure ΔI over a considerable range in q_z to observe the oscillation, which suggests using hard X-rays. A simulation of such a measurement is given in Fig. 2.

The correlation functions we use for simulating the data are taken Ref. [1]; i.e.: $C(X, Y) = \sigma^2[\exp(-(R/\xi)^{2h})]$, where σ is the root mean-square roughness parameter, ξ is the correlation length, and h is the roughness exponent. In principle, one needs three sets of parameters to describe the three different correlation functions C_{SS}, C_{SM}, and C_{MM}. However, it can be shown that the σ associated with C_{SM} is given by $\sigma_{SM}^2 = \frac{1}{2}(\sigma_S^2 + \sigma_M^2)$, where $\sigma_{S,M}$ are associated with C_{SS} and C_{MM}, respectively. We further have assumed that $\xi_{SM}^2 = \frac{1}{2}(\xi_{SS}^2 + \xi_{MM}^2)$.

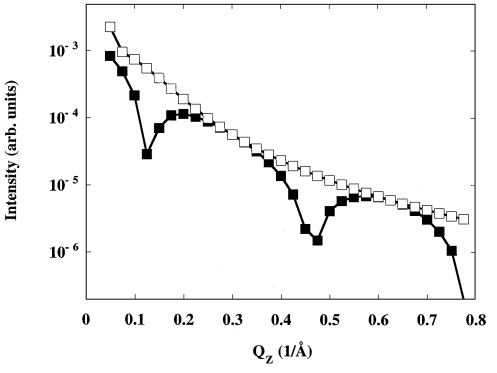

Fig. 2. Longitudinal diffuse scan ($|\Delta I|$ as a function of q_z with $q_x = 0.004$ Å^{-1}), with $\lambda = 1.57$ Å(7.88 keV), with (filled symbols) and with out (unfilled symbols) the presence of a 10 Å dead layer at the surface. Simulation parameters are referred to in the text.

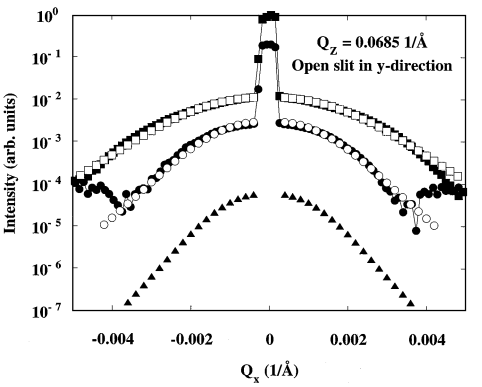

Fig. 3. experimentally measured values of ΔI (filled dots) and $I_+ + I_-)/2$ (filled squares) for a Si/Cu/(400 AA)/$Co_{0.95}$ $Fe_{0.05}$(50 Å)/Cu(30 Å) sample, plotted as a function of q_x, the transverse momentum transfer, at $q_z = 0.0685$ Å^{-1}. The specular peak is located at $q_x = 0$ and was not fitted. A simulation of ΔI is denoted by unmarked squares; a simulation of I_{ave} is denoted by unfilled circles. Triangles denote a simulation of $d\sigma/d\Omega|_{\sigma\to\pi}$. Simulation parameters are referred to in the text.

Our main conclusion, that for $\boldsymbol{M}\|\hat{x}$ there is no diffuse scattering (to leading order in M) in ΔI if the structural and magnetic interfaces are uncorrelated, holds true even if the detector is moved out of the x–z plane, as was done by MacKay et al. [8]. The details of this proof will be supplied in a future publication.

As an example of the use of our formulae for simulations, we present data from a 50 Å thick $Co_{0.95}Fe_{0.05}$ layer capped by 30 Å Cu. The CoFe film was (1 1 1)-textured and was deposited onto a 400 Å thick Cu layer (itself deposited onto a Si wafer) which had been deliberately roughened to study the effects of roughening on the magnetic and structural surfaces [10]. We treated the CoFe layer as having a sharp interface, so that $f_m(q_z) = 1$ in Eq. (8). Displayed in Fig. 3 are experimentally measured values of ΔI and I_{ave} from this sample, for a transverse scan, plotted as a function of q_x, the transverse momentum transfer, at $q_z = 0.0685$ Å^{-1} . The specular peak is located near $q_x = 0$, and the slits along the y-direction were wide enough that the detected intensity was effectively integrated over q_y. This results in the integrals in Eq. (8) being replaced by one-dimensional integrals over x only [1].

Simulations of data are also displayed in Fig. 3. The effects of the capping layer were ignored for simplicity. Because the extinction length of the X-rays was much shorter than the effective thickness of the CoFe obtained at grazing ($\sim 5.0^\circ$) incidence, we treated the CoFe as a semi-infinite block with only a single (upper) surface. The off-diagonal component of the dielectric tensor was obtained from transmission circular dichroism experiments on ultrathin Co films. The $|B|^2$ term in I_{ave} is small,

so that the diffuse data for I_{ave} was almost independent of the MM correlation function. The quadratic term C in Eq. (2) was set to zero as discussed earlier.

Both ΔI and I_{ave} were simulated using the formulae in Eq. (14) with $C = 0$, and are displayed in Fig. 3 (this was the case by treated by Hannon et al.) [6]. The shape of the curves were best simulated with a SM correlation length $\xi_{SM} = 1450$ Å, a SS correlation length $\xi_S = 1040$ Å, [from which can deduce a purely magnetic correlation length $\xi_M = 1770$ Å,] and roughness exponents of $h = 1.0$ in all cases. The structural and magnetic roughnesses were set to be $\sigma_{SM} = 10$ Å and $\sigma_S = 10$ Å, respectively, yielding $\sigma_M = 10$ Å. Our calculations gave a ratio of ΔI to I_{ave} which was, at $q_x = 0.0002$ Å^{-1}, roughly $\frac{7}{4}$ times larger than the experimental value (the simulation of ΔI displayed in Fig. 3 has been divided by this factor of $\frac{7}{4}$). In calculating this ratio, we have allowed for incomplete polarization of the beam. We attribute this discrepancy to a combination of factors: reduction of the magnetic moment in the ultrathin Co film causing a reduction in the off-diagonal element of the dielectric tensor, the presence of a 'dead' layer at the interface, which will reduce the size of ΔI *via* the factor $e^{iq_z\Delta}$ in Eq. (14), and the inherent limitations in the BA.

Also displayed in Fig. 3 is a simulated transverse scan involving $d\sigma/d\Omega|_{\sigma\to\pi}$, which is the cross-section for scattering from σ to π polarization. $d\sigma/d\Omega|_{\sigma\to\pi}$ is proportional to $S_{mm}(\boldsymbol{q})$ and so yields direct information about the magnetic surface, but is several orders of magnitude smaller than ΔI.

In conclusion, we have described a general method for calculating both specular and diffuse XRMS in the BA, where the sample can be treated as having separate, but correlated, rough, magnetic and structural surfaces. The leading contribution to the diffuse component in ΔI is non-zero only if the magnetic and structural roughnesses are correlated, for $\boldsymbol{M}$ in the plane of the sample. We have given expressions for the scattering amplitudes in the linear (σ, π) basis. We have shown that interesting physical parameters may be extracted from measurements of ΔI and I_{ave}. We find that $d\sigma/d\Omega|_{\sigma\to\pi}$ is several orders of magnitude smaller than ΔI, making direct measurement of the diffuse magnetic scattering difficult.

Work at ANL was supported by the US DOE BES-31-109-ENG-38.

References

[1] S.K. Sinha, E.B. Sirota, S. Garoff, H.B. Stanley, Phys. Rev. B 38 (1988) 2297.
[2] Z.-P. Shi, P.M. Levy, J.L. Fry, Phys. Rev. B 49 (1994) 15159.
[3] P. Beliën, R. Schad, C.D. Potter, G. Verbanck, V.V. Moshchalkov, Y. Bruynseraede, Phys. Rev. B 50 (1994) 9957.
[4] J.P. Hannon, N.V. Hung, G.T. Trammell, E. Girdau, M. Muller, R. Rötter, H. Winkler, Phys. Rev. B 32 (1985) 5068.
[5] A. Fasolino, P. Carra, M. Altarelli. Phys. Rev. B 47 (1993) 3877.
[6] J.P. Hannon, G.T. Trammell, M. Blume, D. Gibbs, Phys. Rev. Lett. 61 (1988) 1248.
[7] D. Gibbs, D.R. Harshman, E.D. Isaacs, D.B. McWhan, C. Vettier, Phys. Rev. Lett. 61 (1988) 1241.
[8] J.F. MacKay, C. Teichert, D.E. Savage, M.G. Lagally, Phys. Rev. Lett. 77 (1996) 3925.
[9] J.W. Freeland, V. Chakarian, K. Bussmann, Y.U. Idzerda, H. Wende, C.-C. Kao, J. Appl. Phys. 83 (1998) 6290.
[10] J.W. Freeland, V. Chakarian, K. Bussmann, Y.U. Idzerda, H. Wende, C.-C. Kao, unpublished.
[11] C. Kao, J.B. Hastings, E.D. Johnson, D.P. Siddons, G.C. Smith, Phys. Rev. Lett. 65 (1990) 373.
[12] C.-C. Kao, C.T. Chen, J.B. Hastings, E.D. Johnson, D.P. Siddons, H.J. Lin, G.H. Ho, G. Meigs, J.-M. Brot, S.L. Hubert, Y.U. Idzerda, C. Vettier, Phys. Rev. B 50 (1994) 9957.
[13] M. Blume, J. Appl. Phys. 57 (1985) 3615.